The Spreading and Penetration Mechanism of Aqueous Ink into Synthetic Nonwoven Fabrics

Hitomi Hamada* and Douglas W. Bousfield**

Keywords: Darcy's law, ink, nonwoven fabrics, penetration, spreading

Abstract

The mechanism of ink penetration and setting on paper determines the production rate and influences the final print quality. To develop inks and papers for inkjet and flexographic printing, it is important to quantify the degree of ink penetration and ink-dot spreading; the resolution of print is determined by spreading. The final position of ink pigments determines the ink density and the resolution of the printed product.

The ink penetration rates in the thickness direction into nonwoven fabrics were characterized with a Bristow absorption wheel. The radial spreading behavior of micro ink drop onto nonwoven fabrics was measured by capturing images using a microscopic video camera. The spreading rates of the ink-dot radius on the sheets were determined. One- and three-dimensional models based on Darcy's law were applied to predict the ink radial spreading and the penetration into the nonwoven fabrics. The model links the void fraction, pore size, contact angle and the permeability coefficients of the substrates to the ink spreading radius and penetration depth. The results showed a high correlation between the experimental data and the predicted results in the both radial and thickness directions; however in a few cases, the absorption rates were different than expected. The results demonstrate that a combination of the contact angle and the permeability control spreading and penetration of ink. The three-dimensional model could predict liquid spreading and penetration rates into porous media such as synthetic nonwoven sheets.

Introduction

The mechanisms of ink penetration and setting on porous materials such as paper for all kinds of printing methods determine the rate of printing and influence the final quality of the print. Recently, not only coated and uncoated papers but also nonwoven fabrics, synthetic fiber paper and films have been

---

*Research Institute, National Printing Bureau of Japan, 6-4-20 Sakawa, Odawara, Kanagawa 256-0816, JAPAN
**Department of Chemical and Biological Engineering, University of Maine, 5737 Jenness Hall, Orono, ME 04469-5737, USA

used as materials for printing. The surface characteristics of these substrates influence the ink setting rate and quality of printing, but the relationship between the final pigment deposition and the rate of absorption has not been quantified.

The liquid flow in a porous substrate has been shown, in many cases, to follow Darcy's law that states that the rate of flow is proportional to the pressure gradient and inversely proportional to viscosity. Much work has been done in the area of modeling fluid motion in porous media. If the pressure driving force is given by the Laplace equation, and the resistance to flow is described by the flow in a capillary, the Lucas-Washburn equation is found to describe the behavior; this equation is based on a series of parallel capillaries all of the same radius (Dullien, 1992). Often, various correction terms are used to fit the results to experimental data. Darcy's law combined with the Laplace equation was applied to predict the absorption rates in the thickness direction into nonwoven fabrics for aqueous and solvent inks (Hamada et al., 2008), but radial spreading was not considered.

The spreading of drops into thin paper substrates was described by Gillespie (1958). Absorption into thick porous substrates has also been studied, for example by Alleborn and Raszillier (2004a, 2004b); a distinction was made between saturated and unsaturated media. When a bulk source of the drop is taken away, spreading can still occur in unsaturated media. Allenborn and Raszillier (2006) modeled the flow in the media in combination with the drop dynamics. These models require numerical methods to obtain solutions.

Pore network models have been advanced to describe absorption. A model by Bousfield and Karles (2004) is based on the pore connectivity and pore size was proposed that seems to give good comparison with experiments. Schoelkopf et al. (2000) give a network model that accounts for a number of complex features on the porous media. However, models that are based on individual pores and the description of the connectivity are limited to small volume and short times because of the computer time limits. There are limited comparisons between these models and experimental data.

Other models have been proposed that look at porous media as volumes that can have different properties in different regions; individual pores are not described but an average contact angle, void fraction and permeability is assumed for each region. A three-dimensional model that describes the flow in layered porous media has been described (Bousfield, 2003). The model could predict some sets of experimental data for a coating layer on a paper, measuring the properties of each separately. The Darcy's permeability and the capillary force were combined together for the radial absorption modeling into porous media (Shen, 2005).

In this study, the radial spreading and the penetration behaviors of aqueous ink into three nonwoven fabrics were measured. The fabrics were characterized in terms of pore size, pore volume, contact angle, and permeabilities. The spreading and penetration rates were predicted using with models based on Darcy's law.

Material and Methods

Samples

Three kinds of synthetic nonwoven fabrics were used. The sheet named PVA (12 g/m^2) was made from polyvinyl alcohol (PVA) fibers by a wet process. Another sheet named PP-A (15 g/m^2) was made from polypropylene (PP) fibers and polyvinyl alcohol fibers mixed. The sheet named PP-AC (18 g/m^2) was coated with acrylic latex (Nippon Zeon, Japan) on the PP-A sheet.

A pigment type aqueous ink for flexographic printing (T&K TOKA, Japan) was used for our measurements. The ink is composed of magenta pigment, isopropyl alcohol, resin and water.

Characteristics of nonwoven sheets

The pore volume of nonwoven sheets was determined by the silicon oil void test. Silicon oil was applied to the samples to ensure that they were saturated with oil. The oil was wiped from the surface. The void fraction was calculated from the area and weight of the samples before applying the oil and the weight of oil saturated samples.

The contact angle of water on the nonwoven sheets was measured. After dropping water on the nonwoven sheet, a camera recorded the contact angle change of the liquid drop on the substrate every 10 msec for 300 msec.

A mercury porosimeter (Auto Pore IV 9500, Micromeritics Instrument Co.) was used to determine the pore sizes in the nonwoven sheets. The roughness of the sheet surfaces was evaluated by measuring the surface profile of each sheet using a confocal laser scanning microscope (CLSM).

Darcy permeability coefficients

The permeability coefficient in the thickness direction, K_t, was obtained by measuring the rate of water flowing through a given area, $d(V/A)/dt$, of the sample with known pressure based on this form of Darcy's law:

$$\frac{d(V/A)}{dt} = \frac{K_t \Delta P}{\mu T} \qquad (1)$$

where ΔP is the pressure drop across the entire sample and T is the thickness of

the sample that the pressure acts in the flow direction. This flow through experiment was done with air and water.

In the in-plane or radial direction, the permeability coefficient, K_r, was obtained by a capillary rise experiment. A strip of the fabric was brought into contact with the ink. The rise was captured with a camera and three different times. The equation is derived by replacing the pressure gradient in Darcy's law with the Laplace pressure $2\sigma cos(\theta)/R_p$, the length of sheet wetted by an ink capillary rise, L, and integrating with respect to time to obtain:

$$L = \sqrt{\frac{4K_r \cos(\theta)\sigma t}{\mu \varepsilon R_p}} \qquad (2)$$

where θ is the contact angle, σ is the surface tension, μ is the viscosity, ε is the void fraction of the sample and R_p is the average pore radius. The contact angle, void fraction and pore radius were obtained from experiments, while the surface tension and viscosity were assumed to be the same as water for the aqueous ink.

Ink penetration rate

The penetration rates of ink into nonwoven sheets were characterized with a Bristow absorption wheel (Bristow, 1967). A known volume of diluted ink was added to the trough. The inks had to be diluted to enable them to flow easily through the slit at the bottom of the trough. The area of the trace left on the substrate was measured. The contact time between the ink and the substrate was varied by changing the speed of the wheel. In some cases, several layers of the fabric were needed to prevent the "saturation" of the sample even for the shortest times that could be measured. The volume absorbed per unit area was then calculated.

Because the length scale for Darcy's law, in Eq. (1) scales with the volume absorbed as $L = V/(A\varepsilon)$, where ε is the void fraction, the length scale can be eliminated from the equation. After integration with time, the result is

$$\frac{V}{A} = \sqrt{\frac{4K_t \varepsilon \cos(\theta)\sigma t}{\mu R_p}} \qquad (3)$$

where V/A is the ink absorption volume per unit area. This expression is similar to the Lucas-Washburn equation except that the resistance to flow is expressed in a general way, not as a function of pore size.

Real samples have a distribution of pore sizes. There is no clear radius to use in Eq. (3). A simple way to include a distribution of radii is to use the porosity results in different radius size classes. For each size class, the volume of pores is

known from the porosity data. Therefore, a void fraction ε_i can be calculated for each radius size class R_{pi}. The absorption amount is assumed to be a summation of the absorption of each size class as

$$\frac{V}{A} = \sum_i \sqrt{\frac{4K_t \varepsilon_i \cos(\theta)\sigma t}{\mu R_{pi}}} \qquad (4)$$

Even though this expression uses different void fractions for different pore sizes, the same permeability is used. In reality, different values of permeability likely correlate with different pore sizes. The method to describe a pore size distribution in this type of expression is not clear. More work is needed to verify a reliable method to account for a pore size distribution within an expression like this.

Radial spreading

The spreading behavior of an ink drop onto nonwoven fabrics was measured by capturing an image every 20 ms using a microscopic video camera. The changes of ink-dot radius on the sheets were measured.

If the thickness of the substrate below a drop is assumed to be saturated with fluid, the only direction for absorption is radial. By neglecting thickness direction absorption, a simple expression can be obtained. Conservation of volume gives the expression that the radial velocity multiplied by radius is a constant. Using this and Darcy's law expressed in radial direction gives an expression for the spread radius as a function of time. The equations, first given by Shen (2005), were used to predict ink spreading behavior to the radial direction.

$$\lambda t = \frac{R_t^2}{2}\ln\left(\frac{R_t}{R_0}\right) + \frac{(R_0^2 - R_t^2)}{4} \qquad (5a)$$

$$\lambda = \frac{2K_r \cos(\theta)\sigma}{\mu \varepsilon R_p} \qquad (5b)$$

where λ is an effective permeability, R_t is the ink-dot radius at the time, t, and R_0 is initial ink-dot radius. The maximum ink-dot radius, R_m, and the time, t_m, were calculated from the initial ink volume and the void fraction and the thickness of the sheets. After this time, $R_t = R_m (t \geq t_m)$.

Three-dimensional model

In the inkjet printing and flexographic printing situations, the volume of the ink is less than the volume of the paper under the drop. In the experiments, even

with drops as small as a millimeter in diameter, the drop volume is more than the capacity of the paper. Therefore, in the spreading experiments with the applied, drop, the key feature would be drop spreading in the radial direction. In the case of actual printing, both thickness and radial direction spreading is possible.

The model described by Bousfield (2003) is modified to describe both the penetration and radial spreading of a drop on a porous surface. The substrate is divided into equally sized volumes. Figure 1 depicts the calculations. Volumes that are partially full are assigned the Laplace pressure relative to atmospheric. The volumes that are in contact with the drop are assigned atmospheric pressure. Regions in the first layer not in contact with the drop can only obtain fluid from other volumes, not from the face above them. Volumes that are filled have imposed a conservation of mass expression: the net flow in and out of the volume has to be equal. This restriction generates an equation that links the fluid velocities together at every volume that is filled; details are given in Bousfield (2003). These linear equations can be solved with standard matrix manipulations. The model, at present, does not allow for volumes to empty. Also, the calculation is assumed to stop when the volume of fluid in the porous media equals that of the drop. A pore size distribution is assigned here to duplicate the porosimetry data. The models by Alleborn and Raszillier (2004a, 2004b, 2006) have a few features that are better than this description, but the desire here is to see if this simplified description will be accurate.

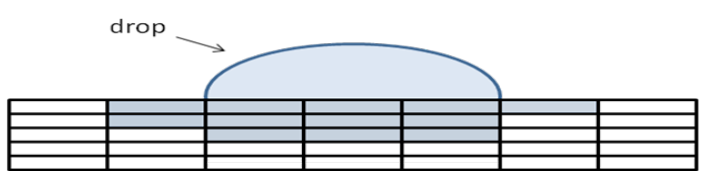

Figure 1. *Drop radial spreading and penetration on porous substrate. The flow between cells is used to predict absorption rates.*

Two different extremes are possible to predict: 1) the penetration in the thickness direction is slow, and the top layers of the material absorb fluid outward from the drop or 2) the fluid penetrates the thickness of the material and moves outward as a column of fluid.

Results and Discussion

Characteristics of nonwoven sheets

Table 1 shows the properties of the nonwoven sheets. In the silicon oil test results, the PVA sheet showed the highest void fraction (ε), while the PP-AC sheet had the lowest value because it was coated with latex. The contact angle (θ) measured at 10 ms is shown in Table 1. The PVA sheet showed the lowest

water contact angle because the PVA fiber is hydrophilic. The PP-A sheet showed the highest water contact angle. This is because polypropylene fiber contained in the PP-A sheet is hydrophobic. Comparing the PP-A sheet with the PP-AC sheet, the water contact angle decreased after coating with acrylic latex and the surface became more hydrophilic. The roughness of the nonwoven sheets is correlated with the standard deviation of the amplitude given by surface profile measurements. The PVA sheet showed the highest standard deviation, which means that the surface of PVA sheet is the roughest.

Table 1. *Measured parameters of substrates.*

		PVA	PP-A	PP-AC
Thickness (μm)		45	58	66
Void fraction	ε	0.44	0.38	0.36
Contact angle	θ	74	90	74
Pore radius (μm)	R_p	18	18	14
Surface profile, standard deviation of amplitude (μm)		13	5.8	9.0
Permeability, thickness, one sheet (m^2 x 10^{12})	K_{t1}	0.9	1.1	0.8
Permeability, thickness, ten sheets stack (m^2 x 10^{12})	K_{t10}	3.3	15	9.2
Permeability, radial (m^2 x 10^{12})	K_r	0.54	3.1	0.2

Two kinds of permeability in the thickness direction were measured; one sheet and ten sheets piled. The hydrophilic PVA sheet showed lower permeability despite of its high void fraction, and the hydrophobic PP-A sheet was the highest permeability in the both directions. This result is hard to understand but must be related to the connectivity of the pores. The result shows that the ten stack thickness direction permeability is found to be almost an order of magnitude larger than the one-sheet permeability. It is expected that the flow rate would decrease by a factor of ten for ten sheets, but in reality, the flow rate did not change. The reason for this result may be that water leaks between sheets during the measurement or the one-sheet permeability may have a large margin of error because of fast water flow. In most cases, the thickness direction permeability is higher than radial direction. This result must be a result of how these sheets, and most paper, is made, by laying down fibers from a suspension. The drainage from the fibers must help keep the thickness direction pores open. However, in the radial direction, the connection and flow paths are constricted. Whatever the cause of this non-uniform permeability, it should be noted that the values are different.

Figure 2 shows pore size distributions in the sheets measured by the mercury porosimeter. It is clear that all samples have a wide range of pore sizes. The average value of pore size, R_p, in each sheet is shown in Table 1. Figure 3 shows

the cumulative pore volume. The each void fraction (ε_i) is shown in Table 2 for each radius size class (R_i) in divided four radius size classes: Zone 1-4 shown in Fig. 3. The pores larger than 60 μm may be an artifact of how these samples are mounted because the sample thickness is in this range. Therefore, it is unclear if these large pores should be included in the prediction of absorption rates.

The uncoated PVA and PP-A sheets have larger pores between 20 and 100 μm of diameter. In the coated PP-AC sheet, there were many smaller pores between 0.1 and 5 μm. This is because larger pores were filled up with the latex. The PP-A sheet showed the highest pore volume, which did not agree with the silicon oil test results. However, the data in the region larger than 100 μm might not be reliable because of the method to hold the sample in the porosimeter.

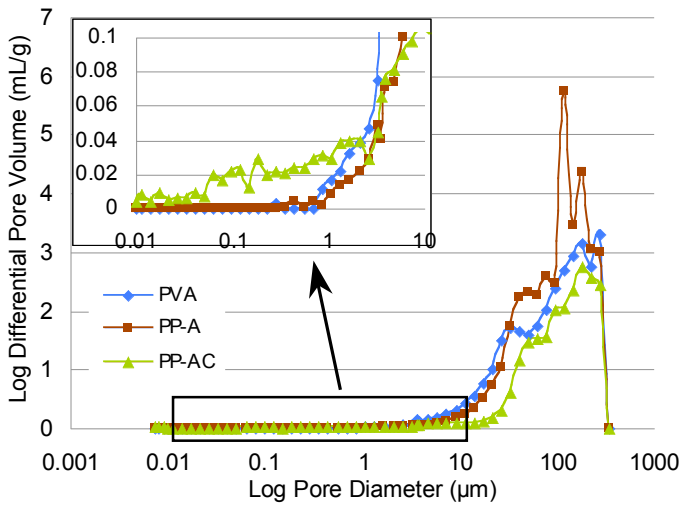

Figure 2. *Pore size distributions in the nonwoven sheets.*

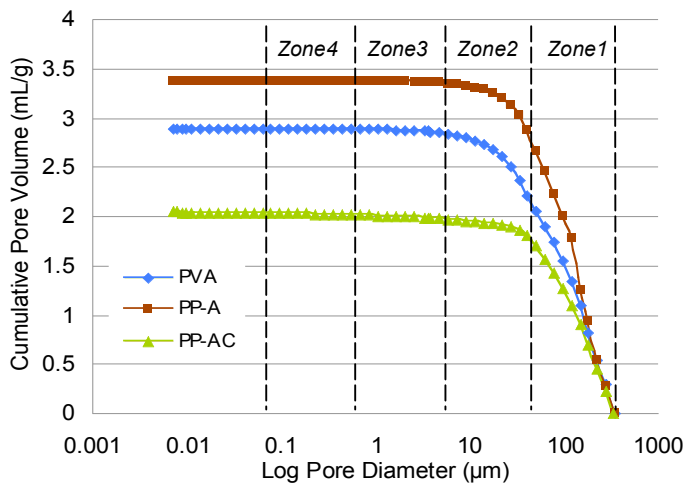

Figure 3. *Cumulative pore volume in the nonwoven sheets.*

Table 2. Void fraction in different radius size classes.

			Zone1	Zone2	Zone3	Zone4
Pore radius	R_i (μm)		64.6	7.62	1.05	0.125
Void fraction	ε_i	PVA	0.666	0.194	0.011	9.0×10^{-5}
		PP-A	0.741	0.124	0.005	1.7×10^{-4}
		PP-AC	0.493	0.046	0.009	0.0055

Ink penetration rate into nonwoven sheets

Figure 4 shows total liquid volume (TLV) transferred to the sheets per unit area by measuring with the Bristow absorption wheel; this volume is also related to the penetration depth of fluid into the sample. Solid lines represent experimental data and dotted lines are the predicted results of Eq. (3). For the prediction, the experimental data of permeability coefficient in the thickness direction of one sheet (K_{t1}), average void fraction (ε), contact angle (θ) and average pore size (R_p) shown in Table 1 and the literature data of water for surface tension and viscosity were used.

The aqueous ink seems to spread over the surface of the PVA sheet and does not penetrate deeply into the sheet because the surface is hydrophilic and the permeability in the thickness direction is low. These results demonstrate that a combination of the contact angle and the permeability control penetration. Comparing the PP-A sheet with the PP-AC sheet, the penetration depth of the ink increases when acrylic latex is used. The ink may penetrate deeply into the PP-AC sheet in regions where there is latex: this sample had ink that penetrated to the bottom of the sheets by CLSM (Hamada et al., 2008).

The results showed a good correlation between the experimental data and the predicted results for the PP-A sheet as shown in Fig. 4. This demonstrates that the model captures the correct relationship between contact angle, pore size and permeability. However, for the case of the PVA and PP-AC sheets, the measured absorption rates were lower than expected. This difference may be caused by ink trapped in the space between the piled sheets, which led to decrease of the absorption depth. According to the surface profiles by CLSM shown in Table 1, the surfaces of PVA and PP-AC sheets were rougher than PP-A sheet. For the predicted results, the low values of absorption rate in PP-A was attributed to the high contact angle. The high values of PVA and PP-AC sheets were attributed to the low contact angle and medium permeability coefficient.

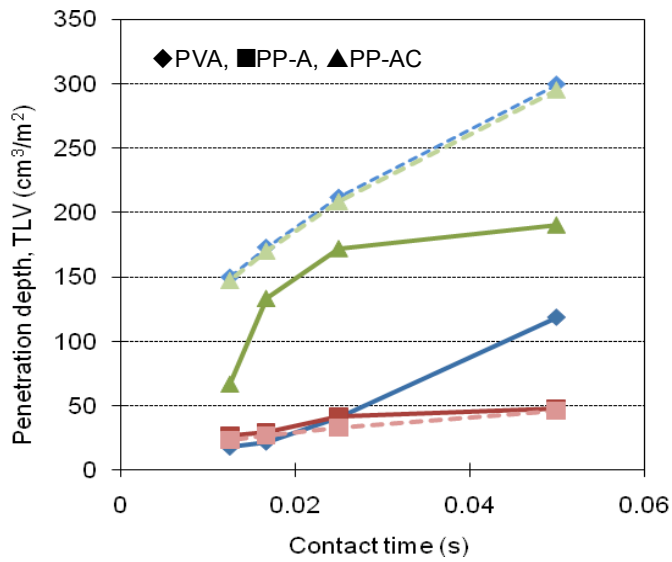

Figure 4. *The thickness direction penetration rates of ink.*
Dotted lines; predicted by Eq(3), K_{t1}, Solid lines; experimental.

The predicted results derived from Eq. (4) are shown in Fig. 5. The each void fraction (ε_i) was calculated for each radius size class (R_i) in divided four radius size classes: Zone 1–4 shown in Fig. 3. The given data shown in Table 2 were assigned to Eq. (4). The permeability coefficient in the thickness direction of one sheet (K_{t1}) was used for this prediction. The result given by a distribution of pore sizes should be accurate and closer to the experimental data, however the predicted absorption rate is again higher than the experimental data. It was twice the previous predicted result derived from Eq. (3). The data in the region of larger pore size by the porosimeter might not be reliable because of sample mounting issues; these artificial large pores would cause the predictions to be

high. If the data of larger region is cut out for the calculation, the result would be closer to the measured values.

If the values of the ten stack permeability (K_{t10}), in table 1 are used, along with Eq. (3), the predicted absorption rate is also higher than what is measured, by a factor of 3–10 as shown in Fig. 5. Errors in viscosity, surface tension, pore size, or pore volume seem unlikely to account for such a difference. For example, if the viscosity were a factor of ten higher, this would reduce the predictions by a factor of the square root of ten, still far from the measured values. There may be a few issues that cause this difference: 1) during the measurement of permeability, water may find preferred channels, 2) during the absorption measurement, fluid is not able to easily transfer from one layer to another, or 3) the internal contact angles that drive the flow are not the same as the measured values at the surface.

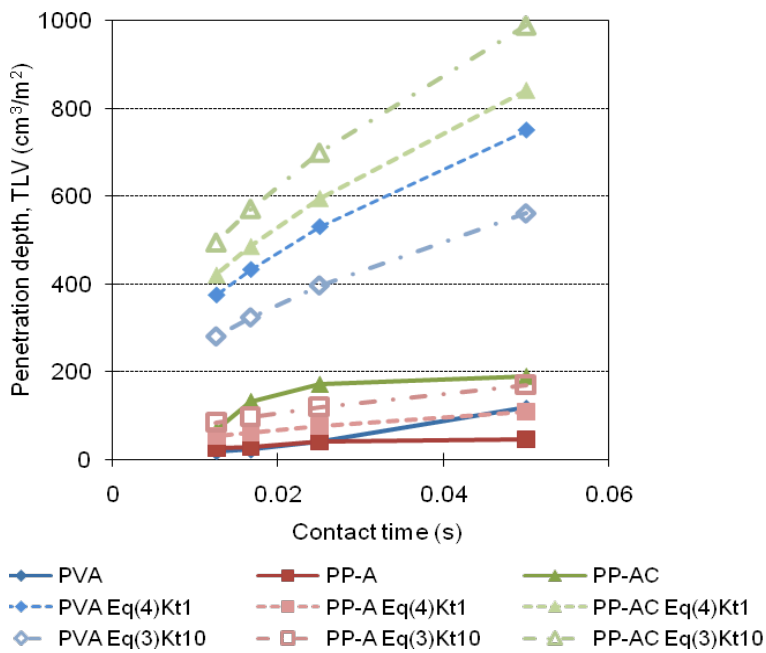

Figure 5. *The thickness direction penetration rates of ink. Dotted lines; predicted, Solid lines; experimental*

Radial spreading rate onto nonwoven sheets

Figure 6 shows the ink drop (1 μL) images on the nonwoven sheets by capturing an image every 20 ms using a microscopic video camera. The initial ink

spreading behavior after contact was observed. In this figure, the each sheet was piled up 10 layers for preventing the saturation of ink. When it was measured for one layer, not piled layers, the spreading rate was faster and the final ink-dot radius was larger than the result of piled sheets. This is because that the ink cannot penetrate into the thickness direction after the saturation in the one layer and spread more in the radial direction.

The initial ink spreading speed was faster on the hydrophilic PVA sheet than the other sheets. The spreading speed on hydrophobic PP-A sheet was the slowest. This shows that the initial spreading speed depends on the contact angle of the surfaces. The shape of ink-dot was approximately circle on the PVA and PP-A sheets; on the other hand, it was close to ellipse on the PP-AC sheet. This would come from uneven surface by coating. The ink penetrated through 4 layers in all nonwoven sheets.

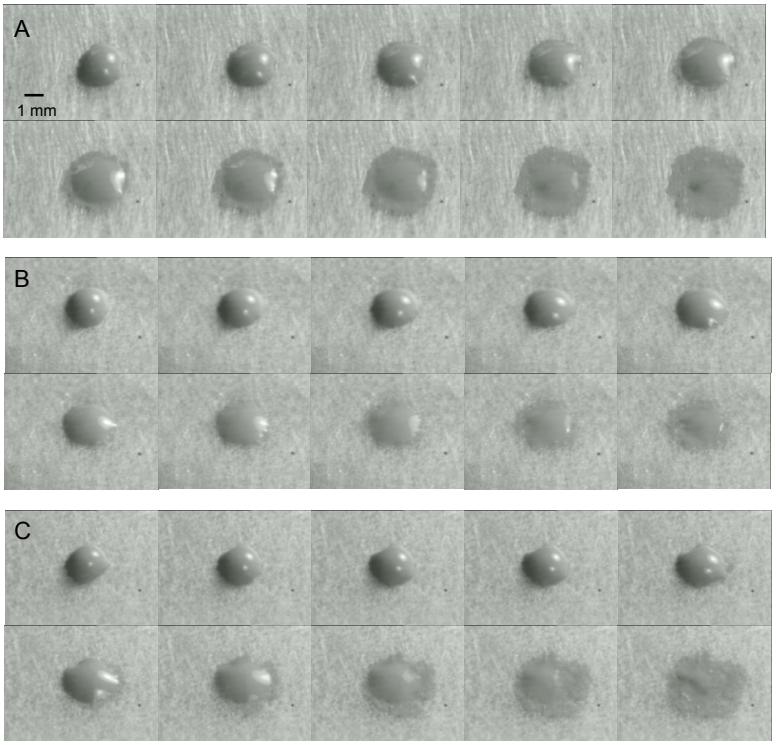

Figure 6. *Ink drop images on the piled sheets captured every 20 ms.*
A: PVA, B: PP-A, C: PP-AC

Figure 7 shows the spreading rates of ink-dot radius on the one layer for each nonwoven sheet measured from the captured images and the predictions using Eq. (5); the solid lines represent experimental data and dotted lines are the

predicted results derived from Eq. (5). For the prediction, the experimental data of permeability coefficient in the radial direction (K_r), average void fraction (ε), contact angle (θ) and average pore size (R_p) shown in Table 1 and the literature data of water for surface tension and viscosity were used.

The aqueous ink spread more over the surface of the PVA and PP-AC sheets than the PP-A sheet in spite of the lower permeability in the radial direction. The high spreading rates in PVA and PP-AC were attributed to the low contact angle and the low rate of PP-AC sheet was attributed to the high contact angle. The experimental data were higher than predicted. This result is likely caused by the ink saturating the sample in the thickness direction in the early times, but at long times, ink is pulled out of the large pores by the fine pores in the radial direction. The sheet was put on a glass slide in our measurements. The excess ink trapped under the bottom side of the sheet after saturation may also encourage the faster spreading in the radial direction.

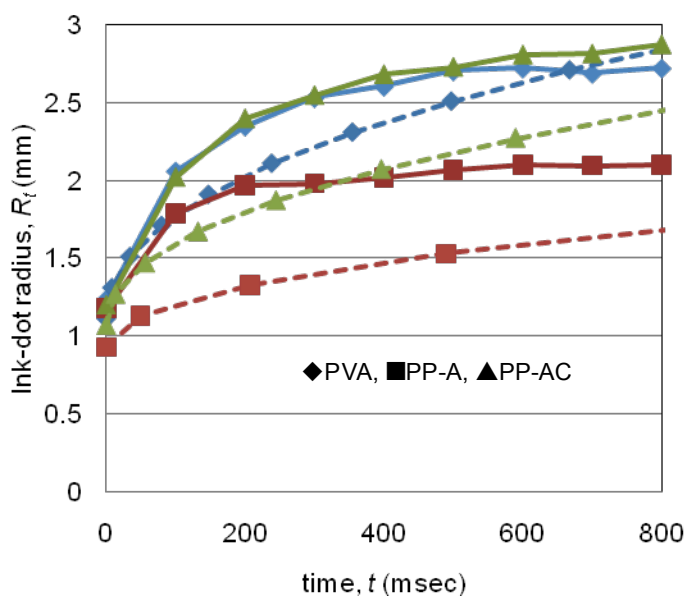

Figure 7. *The radial spreading rates of ink-dot on one sheet. Dotted lines; predicted, Solid lines; experimental*

Figure 8 shows the results on the 10 piled layers of each nonwoven sheet. The predicted results were derived from Eq. (5). The initial spreading rate was slower and the final ink-dot radius was smaller than the previous results with one layer. The ink penetrated into the thickness direction with spreading; it caused the slower spreading. This condition is closer to the real printing method.

The spreading rate was higher on the PVA and PP-A sheets than the PP-AC sheet as the previous result.

For the case of the piled sheets, the result showed a high correlation between the experimental data and the predicted results. The maximum ink-dot radius, R_m, was calculated from the thickness of four piled sheets because the ink penetrated until the 4 layers depth. Only the result of coated PP-AC sheet was a little higher than expected; this result may be caused by the many small pores in this sample that are able to continue the spreading event by emptying larger pores that were under the drop, but are no longer being supplied with fluid from the drop. The results for this sample indicate that the ink was initially absorbed into the sheet through the larger pores and moved slowly to smaller pores. Therefore, the apparent radius of ink-dot was larger than the theoretical value and the radius gradually increased on the PP-AC sheet in the experiment. If the predictions could apply the wide range distributions of pore size, the results may be closer to the experimental data. The properties of the substrates such as contact angle and permeability control the radial spreading rates of ink.

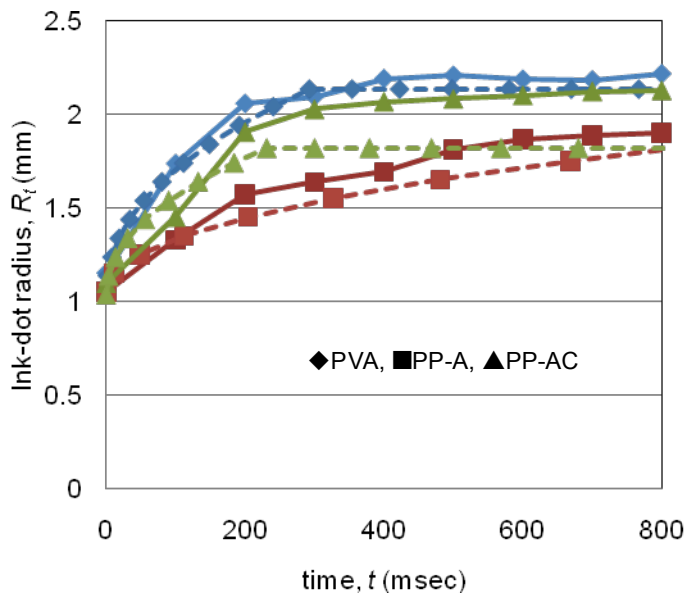

Figure 8. *The radial spreading rates of ink-dot on ten piled sheets. Dotted lines; predicted, Solid lines; experimental*

When the thickness direction permeability, especially stack permeability, was used for the prediction, the predicted equilibrium times were smaller than the results given by the radial direction permeability. This comes from the higher permeability of the substrates in the thickness direction than the radial direction. The radial spreading predictions were better than the penetration predictions.

Three-dimensional model

The three-dimensional model predicted the radial spreading results well when using the single sheet radial permeability in Table 3. Figure 9 shows the full behavior of the model, comparing the shape of the penetration front at a short and longer time. A pore size distribution was used in the model; this leads to a non-spherical shape of the absorption front. Figure 10 shows the predicted results for the PVA sheet. The results agree quite well with figure 8 when using the radial permeability. However, the predictions are often for less spreading than is measured for the other sheets. The model gives penetration depth information as shown in Figure 9.

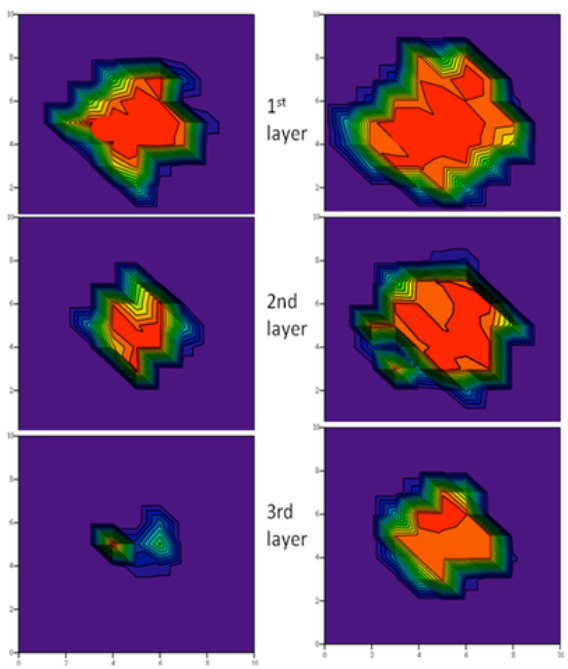

Figure 9. *Prediction for permeability of $5.4x10^{-13}$ m^2, contact angle of 75°, and pore size of 40 microns at two times. The layers are sepearated by 25 microns. The width of the images are 8 mm. The initial drop size is 1 mm diameter. Left column is at 200 ms. The right column of images is at 800 ms.*

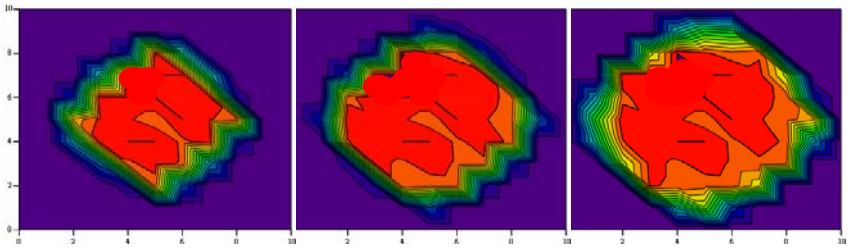

Figure 10. *Top layer for parameters that resemble the PVA sheet, for times of 100, 200, and 300 ms, from left to right. The drop size increases from 1.5 mm to 2 mm in this time scale, starting at 1mm at time zero.*

Even though the three dimensional model gives more information and the correct spreading radius behavior, the simpler expression in Eq. (5) also gives good predictions. This is surprising because of the assumption in the model that the substrate is saturated in the thickness direction.

Conclusion

The ink spreading and penetration rates into three substrates were predicted, within expected accuracy, by various models based on Darcy's law: predictions for radial spreading were better than penetration. A range of permeabilities, contact angles, pore sizes and void fractions are covered. The permeability in the radial direction is different from the thickness direction on the porous media such as papers and nonwoven fabrics. By applying the permeability for the correct direction of absorption, the predictions for the ink radial spreading and penetration rates became increasingly accurate. The three dimensional modeling for ink absorption into porous media could be possible using the model combined the radial and thickness directions.

References

Alleborn, N. and Razillier, H.

2004a, "Spreading and sorption of droplets on layered porous substrates," *J. Colloid Interface Sci.*, 280, pp. 449–464.

2004b, "Spreading and sorption of a droplet on a porous substrate," *Chem. Eng. Sci.*, 59, pp. 2071–2088.

Alleborn, N. and Razillier, H.

2006, "Dynamics of films and droplets spreading on porous substrates," *Proc. Technical Association of Pulp and Paper Advanced Coating Fundamentals Symposium*, Tappi Press, Atlanta, GA.

Bousfield, D.W.

2003, "Three dimensional modeling of short time fluid absorption in layered porous materials," *Preprints, 5th International Paper and Coating Chemistry Symposium* (Montreal, Canada 2003) pp. 253–258.

Bousfield, D. W. and Karles, G.
2004, "Penetration into three-dimensional porous structures," *J. Colloid and Inter. Sci.,* 270: 396.

Bristow, J.A.
1967, "Liquid Absorption into Paper during Short Time Intervals," *Svensk Papperstidning,* 19 (15), pp. 623–629.

Dullien, F. A. L.
1992, *Porous Media—Fluid Transport and Pore Structure 2.ed,* Academic Press.

Gillespie, T.
1958, "The spreading of low vapor pressure liquids in paper," *J. Colloid Sci.,* 13, pp. 32–50.

Hamada, H., Bousfield, D. W. and Luu, W. T.
2008, "The absorption mechanism of aqueous and solvent inks into synthetic nonwoven fabrics," *24th International Conference on Digital Printing Technologies Proceedings* (NIP24, Pittsburgh, PA 2008), pp. 549–552.

Schoelkopf, J., Ridgway, C. J., Gane, P. A. C., Mattews, G. P. and Spielmann, D. C.
2000, "Measurement and network modeling of liquid permeation into compacted mineral blocks," *J. Colloid Interface Sci.,* 227, pp. 119–131.

Shen, Y.
2005, "A liquid bridge probe to characterize coating uniformity," Thesis for the degree of doctor of philosophy (University of Maine, 2005).